International Journal of Thermofluids 23 (2024) 100759

Contents lists available at ScienceDirect

International Journal of Thermofluids

journal homepage: www.sciencedirect.com/journal/international-journal-of-thermofluids

A computational search for the optimal microelectronic heat sink using ANSYS Icepak

Sana J. Yaseen [a], Zainab K. Radhi [a], Rana L. Natoosh [a], Raheem Al-Sabur [a], Raad Z. Homod [b,*], Hayder I. Mohammed [c]

[a] Mechanical Engineering Department, College of Engineering, University of Basrah, Basrah, 61001, Iraq
[b] Department of Oil and Gas Engineering, Basrah University for Oil and Gas, Basra, Iraq
[c] Department of Cooling and Air Conditioning Engineering, Imam Ja'afar Al-Sadiq University, Baghdad, Iraq

ARTICLE INFO

Keywords:
ANSYS-Icepak, Fin arrangements
Efficient heat dissipation
Pressure drop

ABSTRACT

The efficient thermal management of microelectronic devices is crucial for their reliability and performance. Heat sinks, particularly those with inline and staggered fin arrangements, are vital in achieving this goal. This study leverages the advancements in computational fluid dynamics (CFD) software to explore the optimal heat sink design for microelectronic devices. While prior research has extensively investigated heat sink design, this work offers novelty by employing ANSYS Icepak software for simulations. This approach enables a comprehensive thermal performance and pressure drop analysis for two distinct fin cross-sections. The study investigates heat sink assemblies housed within a confined space, simulating a realistic operating environment for microelectronic devices. The heat sink is designed to cool a single heat source (chip) mounted on a substrate board. In this paper, two types of fin sections, circular and conical, are studied for two types of fin configurations, inline (IA) and staggered (SA), which are analysed with 36 fins in each case. Each fin is constructed from aluminium and has specified dimensions. Air serves as the cooling fluid within the cabinet, dissipating heat generated by the chip. When comparing the performance of circular pin and cone fins at the same power and mass flow rate, the results indicated that the maximum temperature for circular pin fins is 0.46% of the maximum temperature for cone fins, and they have a higher pressure drop, especially for staggered arrangements. Moreover, the maximum temperature for staggered arrangements is lower than that for inline configurations by a factor of up to 1.17% and 2.035% for circular fins and cone pin fins, respectively. This article focuses on a deep understanding of the design of microelectronic cooling systems. It aims to continuously improve pressure and thermal efficiency by maintaining the minimum limits of pressure drop within the confined space and obtaining the optimal configuration for efficient heat dissipation.

1. Introduction

Microelectronic devices have played a significant role in technological development and have become integral to all civil and military equipment. Since the noticeable increases in their annual use between 1959 and 1983, their growth rate has risen sharply [1]. In the last two decades, reducing the size of microelectronic devices has become a prevalent feature and a measure of product quality and development. This has accompanied a reduction in the spaces available for heat dissipation systems[2]. The development of microelectronic devices has been accompanied by a major development in the heat sink, which are structures that work very effectively to disperse heat, and their development could be of promising importance in the use of microelectronic cooling in the near future [3,4]. The heat sink is characterized by the presence of micro-pin fins that increase the surface area for thermal dissipation, thus increasing its effectiveness and improving its performance. The optimal design of micro-pin fins has become the focus of many studies[5]. Many types of fins, such as square, cone, diamond, cylindrical, triangular, and hexagonal, have been used to discover optimal heat dissipation performance. Recently, other unusual configurations have emerged, such as hydrofoil, trapezoidal, pentagonal, and s-shaped[6]. It has provided valuable results that have contributed to the noticeable development in the efficiency of heat sinks. The fins' design modifications can include the microchannel design parameters (channel cross-section, width, vortex generator, multilayer, bifurcation,

* Corresponding author.
E-mail address: raadahmood@yahoo.com (R.Z. Homod).

https://doi.org/10.1016/j.ijft.2024.100759

Available online 8 July 2024

Nomenclature

List of Abbreviation

CFD	Computational Fluid Dynamics
SA	Staggered Arrangement
3D	Three Dimensional
IA	Inline Arrangement

LIST OF SYMBOLS

ST	The distance between adjacent fins in y direction
Tb	The base height of the heat sink (cm)
W	heat sink width (cm)
Rs	The radius of the base cone
X, Y, Z	Cartesian coordinates
μ	Dynamic viscosity (kg/m.s)
ρ	Density (kg/m^3)
q"	Heat flux (W/m^2)
p	Pressure (N/m^2)
R_{th}	Thermal resistance (°C/W)
S_L	The distance between adjacent fins in x direction
D	fin diameter (cm)
H	fin height (cm)
R_l	radius of the upper cone
u, v, w	Cartesian velocity components (m/s)
k	Thermal conductivity of the material (W/mK)
A	Area of the surface (m^2)
Cp	Specific heat of air at constant pressure (J/kg.K)
T	temperature (°C)
Q	Power (W)
g	Gravitational acceleration (m/s^2)

Sub terms

in	inlet
max	maximum
S	Solid

and porous substrate) and pin fin configurations (density, arrangement, shape, and dimensions)[7]. So, it was found that the way the fins are arranged in the heat sink is of great importance, no less than the number of fins used [8]. The inline arrangement is simple to manufacture, but the pressure loss is increased due to the increased airflow resistance. On the other hand, a staggered arrangement offers a significant benefit by counterbalancing the micro-pin fins [9]. This configuration encourages better airflow and convective heat transfer because it has fewer flow obstructions and improved heat dissipation capabilities. However, the staggered configuration may require more complex manufacturing processes. Positioning the fins within the heat sink is crucial to its overall performance [10,11].

Sparrow et al. [12]studied the heat transfer phases of stepped and inline arrangements and concluded that the inline configuration results in lower heat transfer efficiency and friction factor. Similar results were obtained by Siw et al. [13]. Jalil et al. [14] studied the 3D heat transfer performance of micro-pin fins for inline and staggered arrangements was analysed numerically. They found that the thermal performance of inline micro spindle fins can be improved by 9.3%, compared to 7.9% for stepped configurations. The offset configuration provides slightly better heat transfer performance for the same number of micro-pin fins [15, 16]. By comparing the effect of fin thickness and number when fin height is constant on the thermal performance rate obtained from the central processing unit (CPU), Hosseinpour et al. [17] concluded that the Fin thickness has the most significant effect. Compared to the effect of the number of fins. Tanda et al. [18] presented a study with significant content involving the use of hexagonal fins to study pressure losses and heat transfer for fin exchangers. They used a rectangular channel with rows of diamond-shaped fins, where heat transfer improved by 4.4 times when using equal mass flow rates [19]. They concluded that using hexagonal winglets effectively improved the performance of fin heat exchangers. Ozbalci et al.[20] focused on the power move portions of unendingly staggered finned strategies and affirmed that the inline screw balance strategy makes for a less intense grinding variable and force move limit, Dewan et al. [21]concluded that the intensity move rate is contrarily corresponding to the balance dividing of the round pin-blades. Additionally, heat execution is impacted by warm conductivity and Reynolds number, which should be controlled in the scope of 550–685 for best execution.

In recent years, many solutions have been increasingly used using commercial software such as ANSYS to explore the rate change of thermal performance depending on the arrangement of fins in microelectronic devices [22]where the flow will be partially developed, and the numerical models will be more efficient [23]. Rosli et al. [24]used COMSOL software to simulate the thermal layout of heat sinks equipped with pin fins and found that staggered fins performed better than inline fins, reaching 4.1% in the circular type. Saravanan et al. [25] used FLUENT 16.2 software for 3D numerical analysis to investigate the thermal and fluid flow aspects of a heat sink with triangular pin-fins using different cooling fluids with nanoparticles. They concluded that the heat dissipation rate of the finned heat sink was maximised by 20.31% for ethylene glycol-based nanofluids. Yang and Peng [26] used the SIMPLE computational fluid dynamics algorithm to solve the Navier-Stokes equations to study composite heat sinks' thermal and hydraulic performance and compare them with plate-fin heat sinks. They found that the thermal resistance of pure plate-and-fin heat sinks was higher than that of composite, which included plate fins with some pins between the plates. Abdelmohimen et al. [27]used CFD to compare impinging and parallel flow according to the thermal output performance, pressure drop, and efficiency. They prepared the slides, cutting fins off plate heat sinks to produce configurations of one, two, three, and four slides. They indicated that the impinging flow gives better thermal resistance than parallel flow for all configurations. Zhou and Catton [28] used a 3D CFD model based on the Reynolds-averaged Navier-Stokes equations to examine the energy dissipation and pressure drop of 22 finned plate heat sinks. They found through numerical analysis that the elliptical fin heat sink outperforms all other varieties of pin fin heat sinks. Additionally, statistical approaches were used to study the effect of the fin arrangement method on thermal resistance and pressure drop. Yakut et al. [29]used the Taguchi method to analyse the performance of the hexagonal fins. They concluded that the optimum impacts were seen for the fins at 150 mm height, 14 mm wide and 20 mm height for a flow speed of 4 m/s.

Nahum Y. Godi [30] numerically studied a complex microchannel with innovative fin designs to reduce resistance in a heat sink using complex fin structures. He used three different designs: first, solid cylindrical fins; Second, the solid fins were drilled halfway (50%); the third; The solid fins are 87.5% drilled and mounted on the heatsink. In the simulation configuration, the heat sink has a heat load of 250 W imposed on the bottom wall and a single-phase Reynolds water between 400 and 500 flows in a laminar state by forced convection to remove heat at the bottom and within the surface. fin wall area, while a Reynolds number between 3 and 6 flows convectly through the cylindrical fins to dissipate excess heat outside. The results show that in parallel flow, the heat sink combined with semi-hollow fins outperforms with 27.2% lower resistance, while in counterflow the hollow fins outperform with 19% lower resistance. This work builds upon extensive research on heat sink design, particularly focusing on inline and staggered fin

Table 1
Pin fin Heatsink Geometric Specifications.

Parameter	Dimensions (cm)
Cabinet	6 × 5 × 2
Source	2.2 × 2.2 × 0.1
Heat sink	4 × 4 × 1.7
Fins	Number of fins=36
Base height (t_b)	0.2
Cross section	Circular (D = 0.2); Cone (R_l=0.2, R_s=0.05)

arrangements. However, the ever-evolving landscape of computational tools offers new opportunities for investigation. This study's novelty lies in exploring the optimal heat sink design for microelectronic devices. By leveraging computational simulations, the research aims to identify the best thermal performance configuration for two distinct fin cross-sections while simultaneously controlling pressure drops. This focus on thermal efficiency and pressure optimisation sets this work apart from previous studies that might have prioritised only one aspect.

Anas Al-Khazaleh et al. [4] analysed a MEMS heat sink containing small, corrugated channels integrating circular fins to cool microelectronic chips. The thermal resistance of the proposed MEMS heat sink is only 0.72 and 0.43 of that of the MEMS heat sink containing straight microchannels at Reynolds numbers of 250 and 1250, respectively. This work also analyses the contribution of geometric properties to the behaviour of the proposed MEMS heat sink in terms of the maximum temperature of the microelectronic chip, thermal resistance and pumping capacity as well as those of the microchannel used in the proposed MEMS heat sink in terms of Poiseuille and Nusselt numbers. The maximum microchip temperature and thermal resistance decrease with increasing pumping power, with increasing capacitance, pin fin diameter and hydraulic diameter of microchannel as well as with decreasing wavelength. The Poiseuille and Nusselt numbers increase with increasing amplitude, fin diameter and hydraulic diameter as well as decreasing wavelength.

Mohamed Daadoua et al. [31] experimentally studied the pressure drop and heat transfer characteristics in a small channel heat exchanger.

Table 2
CFD model parameters settings.

parameter	description
Dimension	3D
Near-wall	Stander wall functions
Co-flow-inlet	Velocity inlet
outlet	Pressure outlet
Viscous model	Realisable k-ϵ Pressure-based
Solver type	Steady, Axisymmetric, Implicit

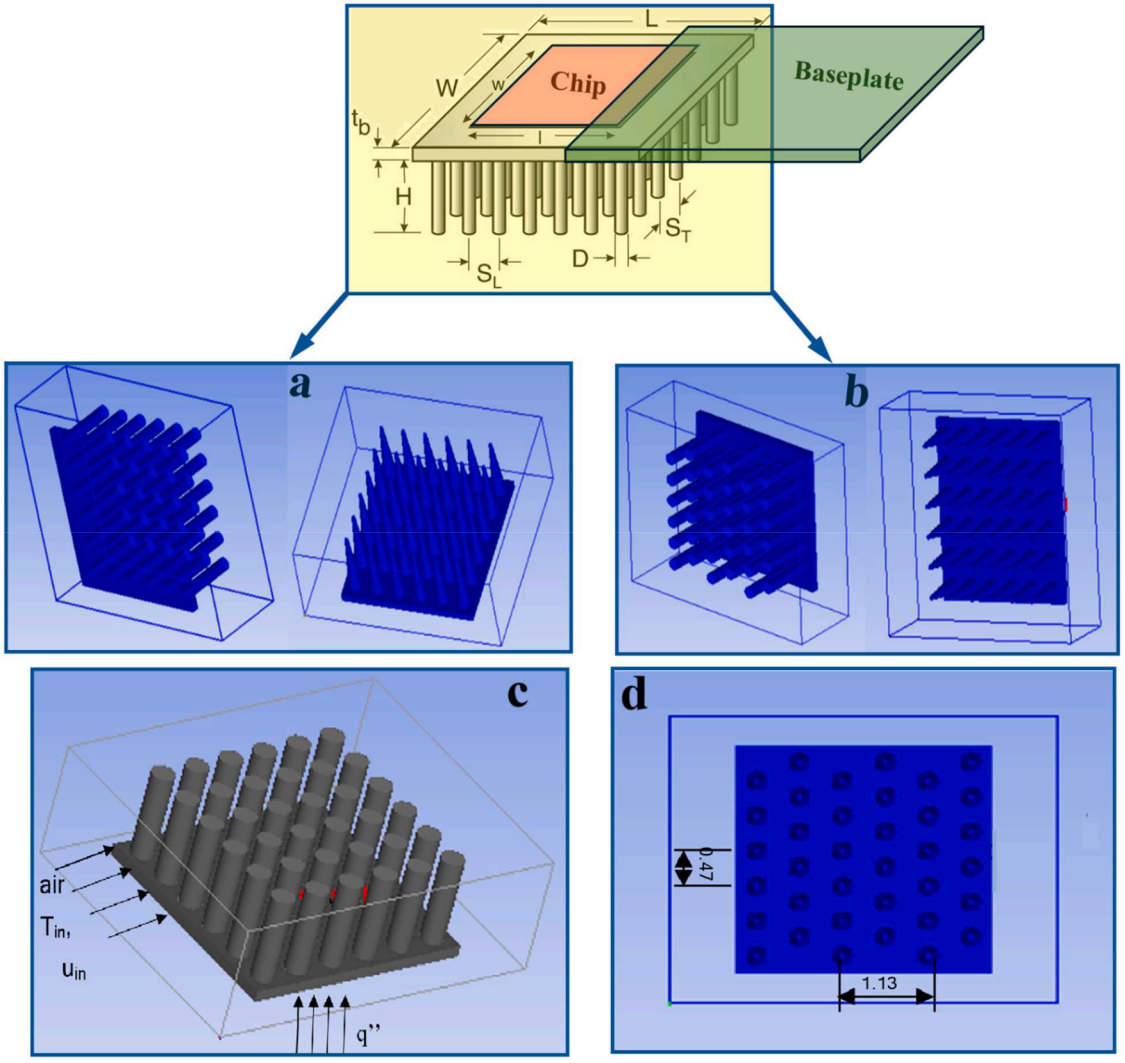

Fig. 1. Schematic diagrams of the heat sink with circular and conical fins: (a) represent the configuration of IA, (b) represent the configuration of SA, (c) and (d) represent the boundary conditions and dimensions.

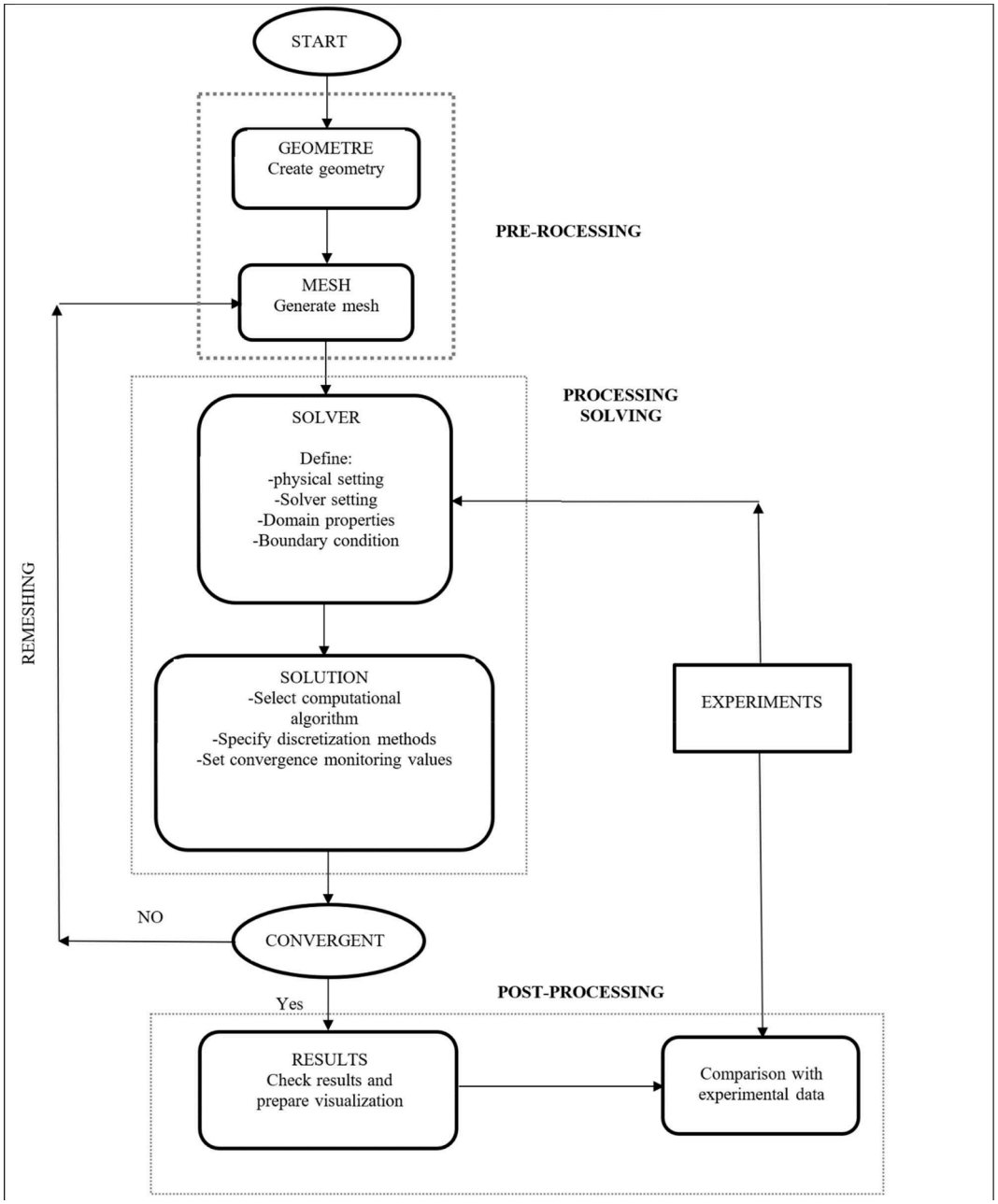

Fig. 2. Flow chart of the numerical solution by ANSYS-Icepak.

Table 3
CFD boundary conditions (input parameters).

parameter	Value
V_{in}	0.1 m/s
T_{in}	298 K
Power	8 W
All the cabinet surfaces are isolated except the inlet and outlet surfaces.	

Table 4
The mesh parameters.

Circular fins	Number of nodes	285,155
	Number of cells	265,075
Cone fins	Number of nodes	399,188
	Number of cells	414,765

Experimental tests were carried out on a small channel with smooth and compact circular fins. The experimental study of pressure drop includes a Reynolds number ranging from 100 to 1900 for hot water and a Reynolds number ranging from 500 to 10,000 for hot air. Hot fluid flows through a channel arranged in line with a 1750-pin fin, while cold fluid flows through a smooth channel. The increase in flow rates led to an increase in pressure losses and heat transfer coefficients. When using a finned surface instead of a smooth surface, the overall heat transfer coefficient (U) increased by 190% when using water as the heat transfer fluid (HTF), and the same coefficient increased by 42% when using air as a heat transfer fluid. fluid. Coolant.

This study is based on extensive research in heat sink design, particularly inline and staggered fin configurations. This research is distinguished from previous ones by focusing on improving the efficiency of heat dissipation and controlling pressure drop by using computational simulations of two distinct cross-sections of the fin.

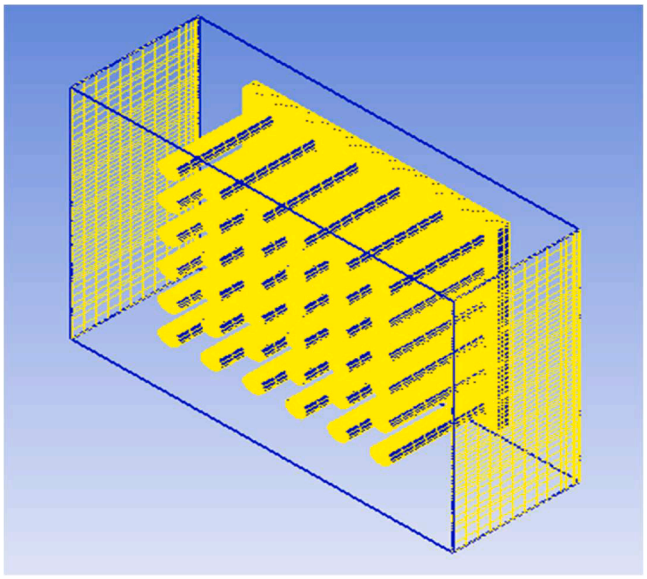

Fig. 3. 3D computational quadratic mesh of the domain.

2. Methodology

2.1. Model description

This study uses computational analysis to investigate the thermal performance of a heat sink assembly housed within a cabinet. The heat sink is designed to cool a single heat source (chip) mounted on a substrate board. The heat sink incorporates 36 fins arranged in two configurations: inline (IA), where the fins are arranged at equal distances from each other, and staggered (SA) arrangements, where the fins on the even number zones are shifted by one-half of the fin spacing. ANSYS-Icepak software serves as the primary tool for the numerical analysis of the heat sink cooling system [32,33]. This software utilises the FLUENT solver, a robust computational fluid dynamics (CFD) package, to perform coupled thermal and fluid flow simulations. As detailed in Table 1, each model within the study consists of the following components:

- Heat Source (Chip): The chip, representing the heat source, has dimensions of 2.2 cm × 2.2 cm × 0.1 cm.
- Heat Sink: The heat sink base, constructed from aluminium, measures 3 cm × 3.5 cm × 2 cm and houses the chip on the substrate board.
- Cabinet: The rectangular cabinet, designed to enclose the heat sink assembly, has dimensions of 6 cm × 5 cm × 2 cm.
- Heat Sink Fins: Each fin within the heat sink is 1.5 cm in height and has a radius of 0.16 cm.

A visual representation of the designed cabinet and heat sink geometry can be found in Fig. 1. Air is employed as the cooling fluid within the cabinet, facilitating heat transfer from the heat sink to the surrounding environment. The chip generates a constant heat load of 8.0 W, simulating realistic operating conditions. By analysing the thermal performance of the heat sink configurations under these defined conditions, the study aims to identify the optimal arrangement (inline vs. staggered) for efficient heat dissipation from the chip within the confined space of the cabinet.

The Realistic $k-\varepsilon$ turbulence model was chosen for its improved

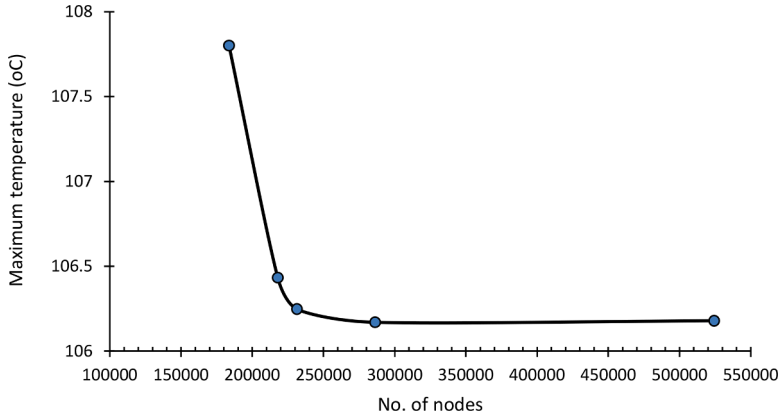

Fig. 4. The maximum source temperature vs. number of nodes.

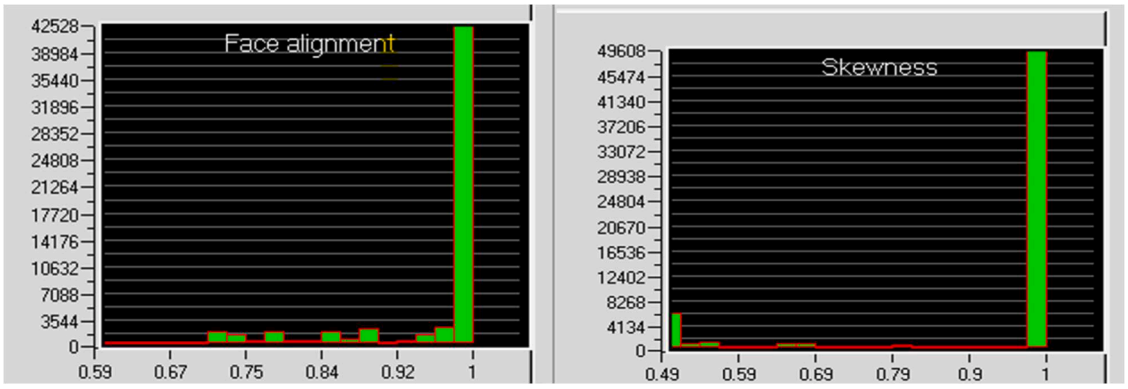

Fig. 5. The present study's face alignment'' and ''skewness values.

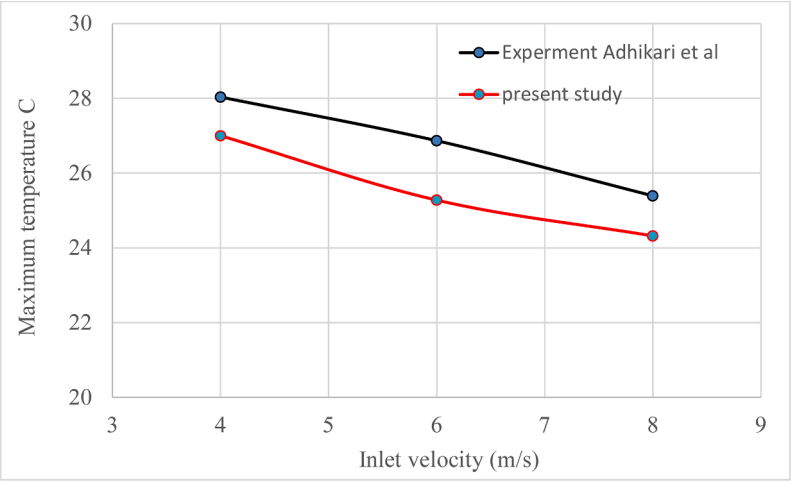

Fig. 6. Comparison of the present numerical study with experimental results of Adhikari et al. [37].

Table 5
Validate the results of this method and Rosli et al. [24].

Arrangement	Source Temperature [24]	Source Temperature (Current Study)	error %
Inline (IA)	107.43 °C	106.474 °C	0.898
Staggered (SA)	101.85 °C	101.662 °C	0.180

accuracy, robustness, and physical realism in predicting turbulent flows, especially in complex scenarios and near walls. Its versatility, extensive validation, industry acceptance, and computational efficiency made it a suitable and reliable choice for accurately capturing turbulent flow phenomena in the study (Table 2).

This study explores the complex airflow dynamics within a cabinet that contains a heat sink. The complexity emerges due to the simultaneous occurrence of many heat transport pathways. Heat transfer occurs in the limited area through a combination of convection and conduction, resulting in a complex process with multiple layers. Convection heat transfer involves the movement of heat through the fluid surrounding the heat sink and cabinet, while conduction refers to heat transfer through the solid components.

In this study, energy equations were used to simulate the movement of heat throughout the system. In contrast, Navier-Stokes equations were the basis for a 3D numerical solution to describe the intricate flow patterns inside the cabinet. The equations thoroughly examine heat transfer phenomena in conjunction with the carefully crafted finite-difference framework. The continuity equation forms the foundational basis for the simulations, providing a detailed representation of the system's thermal and turbulent flow characteristics. Moreover, the solution included assumptions to simplify the solution of energy and momentum equations shown in Fig. 2, which included:

- The flow within the cabinet is assumed to be three-dimensional, considering the potential fluctuations in all three spatial directions (x, y, and z).
- Incompressible flow refers to a situation in which the fluid's density remains constant during the simulation, disregarding any effects that pressure changes may have on it.
- Steady-state flow presumes that the flow patterns and thermal conditions within the cabinet remain unchanged over time.
- Laminar flow refers to fluid motion characterised by smooth and distinct layers, with little mixing between neighbouring levels.
- The no-slip requirement is enforced along the cabinet and heat sink walls, meaning the fluid velocity at the wall is zero.
- The properties of the liquid coolant and the solid components do not change with any temperature change.
- The impacts of radiation heat transmission, energy dissipation within the fluid, and the influence of gravity are deemed insignificant for this particular analysis.

After containing the specified hypotheses, the 3D governing equations enclose the continuity, momentum, and energy equations. These equations can be described below [34]:

$$\frac{\partial u}{\partial x}+\frac{\partial v}{\partial y}+\frac{\partial w}{\partial z}=0 \tag{1}$$

Momentum in x, y and z directions, respectively, are:

$$u\frac{\partial u}{\partial x}+v\frac{\partial u}{\partial y}+w\frac{\partial u}{\partial z}=-\frac{1}{\rho}\frac{\partial P}{\partial x}+\frac{\mu}{\rho}\left(\frac{\partial^2 u}{\partial x^2}+\frac{\partial^2 u}{\partial y^2}+\frac{\partial^2 u}{\partial z^2}\right) \tag{2}$$

$$u\frac{\partial v}{\partial x}+v\frac{\partial v}{\partial y}+w\frac{\partial v}{\partial z}=-\frac{1}{\rho}\frac{\partial P}{\partial y}+\frac{\mu}{\rho}\left(\frac{\partial^2 v}{\partial x^2}+\frac{\partial^2 v}{\partial y^2}+\frac{\partial^2 v}{\partial z^2}\right) \tag{3}$$

$$u\frac{\partial w}{\partial x}+v\frac{\partial w}{\partial y}+w\frac{\partial w}{\partial z}=-\frac{1}{\rho}\frac{\partial P}{\partial z}+\frac{\mu}{\rho}\left(\frac{\partial^2 w}{\partial x^2}+\frac{\partial^2 w}{\partial y^2}+\frac{\partial^2 w}{\partial z^2}\right) \tag{4}$$

Energy equation:

$$u\frac{\partial T}{\partial x}+v\frac{\partial T}{\partial y}+w\frac{\partial T}{\partial z}=\frac{k}{\rho Cp}\left(\frac{\partial^2 T}{\partial x^2}+\frac{\partial^2 T}{\partial y^2}+\frac{\partial^2 T}{\partial z^2}\right) \tag{5}$$

"T" and "P" are the fluid's temperature and pressure, respectively. The u, v, w, ρ, μ, C_p and k are the fluid's velocity, density, viscosity, Specific heat at constant pressure and thermal conductivity, respectively. For the solid walls, the energy equation is given by [35]:

$$\frac{\partial^2 T_s}{\partial x^2}+\frac{\partial^2 T_s}{\partial y^2}+\frac{\partial^2 T_s}{\partial z^2}=0 \tag{6}$$

where 's' refers to the solid region.

The heat sink's thermal resistance can be calculated from [35,36]:

$$R_{\text{th}}=\Delta T_{\max}/Q \quad (^{\circ}\text{C}/\text{W}) \tag{7}$$

$$\Delta T_{\max}=T_s-T_{\text{in}} \tag{8}$$

Where $\Delta T_{\max}$ is the temperature difference between the maximum temperature on the fin base and the ambient air temperature, Q is the power supplied.

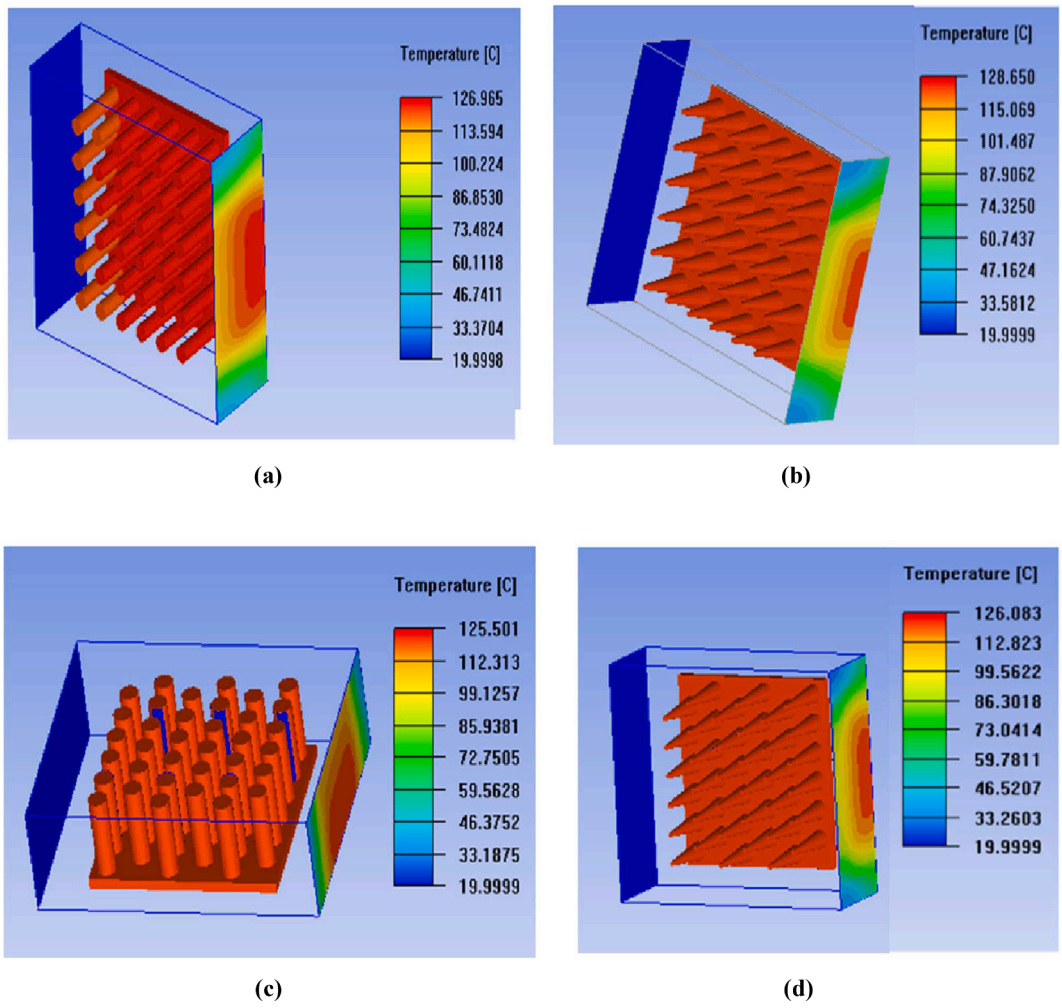

Fig. 7. Temperature contours of (a) IA circular fins (b) IA conical fins (c) SA circular fins, (d) SA conical fins.

2.2. Boundary conditions

This computational analysis uses CFD software to investigate the thermal performance of a heat sink equipped with circular pin fins. The simulation domain encompasses the heat sink and surrounding space. Airflow enters the domain through an upstream boundary positioned sufficiently ahead of the heat sink inlet. This boundary enforces a uniform air temperature (T_{in} = 298 K) and a constant inlet velocity (v_{in} = 0.1 m/s) (Table 3). A pressure boundary condition is applied downstream in the main flow direction (X-direction) at a distance equal to the fin length from the trailing edge. This allows pressure variations at the outlet while maintaining the overall flow rate. All other enclosed surfaces, including the outer boundaries of the heat sink, are designated as no-slip walls with thermal insulation, preventing heat transfer across them. The bottom wall of the heat sink acts as a constant heat source, simulating heat generation within the heat sink itself with a power input of 8 W. An intensity heat flux condition is applied at the interface between the solid heat sink and a presumed coolant flowing within the fins. So, at the connection point, the intensity of the heat flux condition is associated with the temperature gradients in both phases. In contrast, the temperature gradient between the liquid and solid phases is related to the intensity move condition (ks $\partial Ts/\partial y$ = - kf $\partial Tf/\partial y$). At the outlet boundary, the temperature gradient is set to zero ($\partial T/\partial y$ = 0), which means constant temperature conditions. Adopting specific conditions can provide an ideal computational environment for analysing the heat transfer performance of a pin-fin heat sink.

2.3. Grid independence test

In thermal simulations for both inline solid circular pin fins, the mesh size choice plays a crucial role in the accuracy of the results. A hexahedral mesh was generated using (ANSYS-Icepak based on FLUENT) in this study, as shown in Fig. 3. The impact of mesh refinement on the computational results is examined. A key consideration is the total number of mesh cells, as increasing cell count leads to enhanced accuracy but also demands greater computational time and memory resources. Therefore, a mesh dependency study is conducted using meshes of varying sizes (Fig. 4). The influence of mesh refinement on the numerical solutions is evaluated for a case involving 36 inline circular pin fins. The results obtained from these meshes demonstrate that increasing the number of nodes beyond case four does not result in any significant change in the predicted maximum temperature. This suggests that mesh case four represents an optimal balance between accuracy and computational efficiency. It offers a good level of accuracy while maintaining a reasonable calculation time.

In Icepak software, mesh quality is mainly determined by "face alignment", "volume", and " skewness ". A “face alignment” and “asymmetry” closer to 1 mean better mesh quality. The principle of “volume” is a minimum unit volume greater than 1×10^{-12} m^3. The total number of volume cells in the digital mesh of the model, as shown in Fig. 5, "face alignment" and "skewness" are close to 1, and the range of "volume" is 3, 33,333 $\times$ 10^{-007}. In summary, the mesh quality in the present study is good. It is worth noting that the maximum number of iterations is 200 with the convergence criteria of 0.001 and 10^{-7} for the flow and energy,

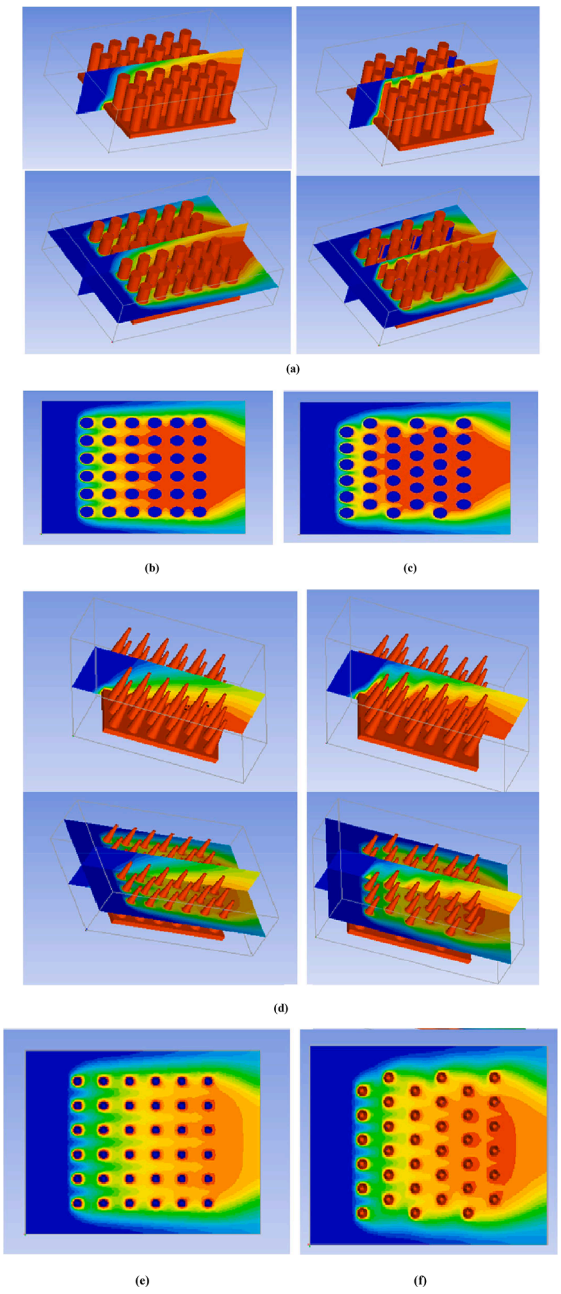

Fig. 8. Temperature contours of (a) circular fins (b) IA &(c) SA, (d) conical fins (e) IA &(f) SA in different planes.

respectively.

2.4. Validation of the numerical method

To validate our numerical work, the results of the present study are compared with the experiment results of Adhikari et al. [37]. Fig. 6 plots the maximum temperature of the heat sink at different inlet velocities. When comparing the results of the present numerical work with Adhikari et al. [37], it can be shown that a good agreement can be obtained with a deviation of less than 3.68%.

Another comparison was also made between the results of our current study and those of another numerical study; both designs had a six-row, six-column structure with a gap of 0.4 cm between pin fins. In the IA model, the heat source's maximum temperatures for the two cases were compared, as shown in Table 5. It is noted that there is great agreement between the two cases. The SA arrangement strongly correlated with the reference data, with only a 0.18% error. However, the IA model indicated a somewhat higher departure, with a 0.898% inaccuracy. The disparity in the IA findings may stem from variances in production, variations in airflow, or difficulties in measurement. The reduced inaccuracy in the SA configuration indicates that it facilitates more effective heat transmission, potentially resulting from improved flow mixing and expanded heat transfer surface area.

3. Results and discussion

As previously mentioned, this study deals with two types of fins, conical and circular, using staggered (SA) and inline (IA) configurations as shown in Fig. 7. This section reviews the potential effects on thermal efficiency of changing the shape and composition of the fins. The study includes fin geometry's effects on temperature, fin geometry's impact on pressure drop, fin geometry's impact on velocity, and fin geometry's impact on thermal resistance.

3.1. Effect of fin geometry on temperature

Possible effects of fin geometry on temperature can be identified by reviewing the maximum temperatures for both circle and conical fins and for both staggered (SA) and inline (IA) installations. The temperature contours indicate that the maximum temperature was lower in the circular fins than in the conical fins for both arrangements. This can be explained by the difference in surface area in both arrangements, as circular fins are characterized by having a larger surface area, which gives them a higher ability to dissipate heat, and thus their maximum temperature is lower. This result provides a clear impression that heat transfer is directly affected by the shape of the fin and the way it is arranged. In addition, the results also indicate that the stepped design has a lower maximum temperature than the inline arrangement for both types of fins. This phenomenon can be explained by the fact that the overlapping fins significantly obstruct the movement of the fluid passing through them. Thus, the fluid needs a greater distance before reaching the exit (Fig. 7). The extended path travelled by the fluid enhances the overall surface area for heat transfer, leading to better heat dissipation and a lower maximum temperature. This discovery emphasises the significance of including flow route optimisation in the design of heat exchangers in order to maximise heat transfer efficiency.

The effect of circular and conical fin distribution can be shown by plotting the temperature distribution on the fins and heat sink through different planes. Fig. 8 shows a drawing of the temperature distribution for both types of fins (cylindrical and conical), for both types of fins distribution, one time through a plane parallel to the y-axis, another parallel to two contours, and the third through a plane that passes through the centre of the cabinet.

Fig. 9 represents the temperature distribution through a line passing through the centre of the cabinet from the inlet area to the exit, passing through the heat sink. We notice from the figure that the temperature from the entry inlet to approximately 0.01 cm is 295 K and it is the same for both types of fins and for both distributions IA and SA. This is because this region is located before the heat sink, that is, before the fluid reaches the area where the heat source is located. Then the temperatures begin to increase and the effect of the type of fin and the arrangement of the fins appears on the curve behaviour. It can be shown that the fins with circular cross-section and staggered arrangement have the lower temperature value.

3.2. Impact of fin geometry on pressure drop

Fig. 10 illustrates the pressure contours for fin shapes and combinations in their respective dimensions. According to the research findings, conical fins have a lower pressure drop when compared to circular fins. The variance in flow resistance associated with the various fin designs in question is the source of the discrepancy. Improving the

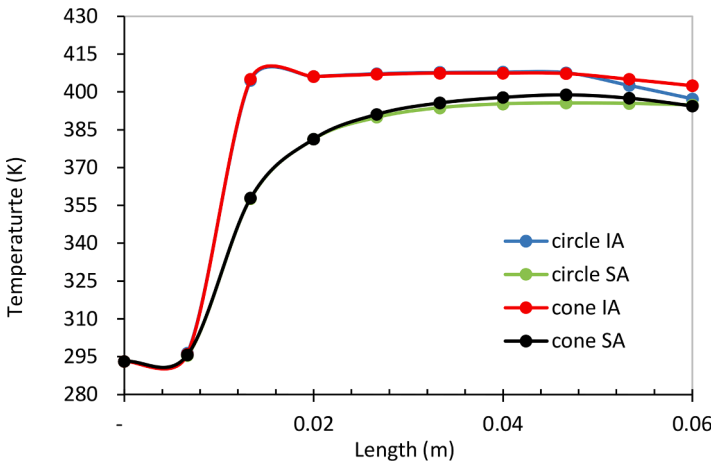

Fig. 9. Temperature distribution along the line passing through the centre of the cabient from the inlet region to the exit, passing through the heat sink.

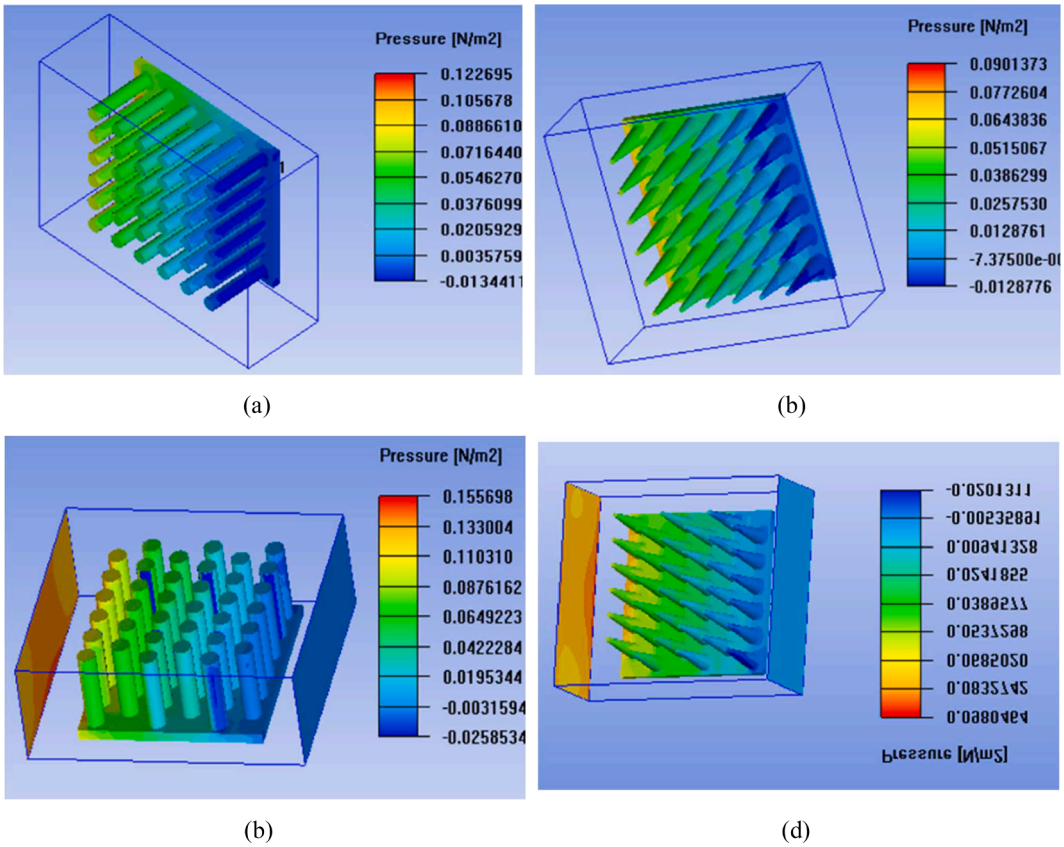

Fig. 10. Pressure contours of (a) IA circular fins, (b) IA conical fins, (c) SA circular fins, (d) SA conical fins.

overall performance of the cooling system of the microelectronic heat sink depends mainly on regulating the pressure drop. Therefore, the shape of the fin and the way it is arranged can accomplish this task perfectly. In comparison, for microelectronic heat sink applications, circular fins can be relied upon because they work to hinder the cooling fluid more and thus have a more significant pressure drop when compared to conical fins that flow through the cooling fluid easily.

3.3. Impact of fin geometry on velocity

Fig. 11 illustrates the velocity contours for fin geometries and configurations in their respective configurations. According to the research findings, conical fins have a lower velocity when compared to circular fins. The variance in flow resistance associated with the various fin designs in question is the source of the discrepancy. It has been observed that the shape of fins may be strategically utilised to regulate the velocity in a cooling system, potentially improving its overall performance. This is something that can be seen.

3.4. Impact of fin geometry on thermal resistance

The effect of fin geometries and configurations on the thermal resistance of a heat sink (Resistance to heat transfer) can be shown in Fig. 12 for both fin geometries and configurations. It can be seen that conical fins have a higher thermal resistance value than circular fins in two cases of IA and SA arrangement. The circular fins have a higher

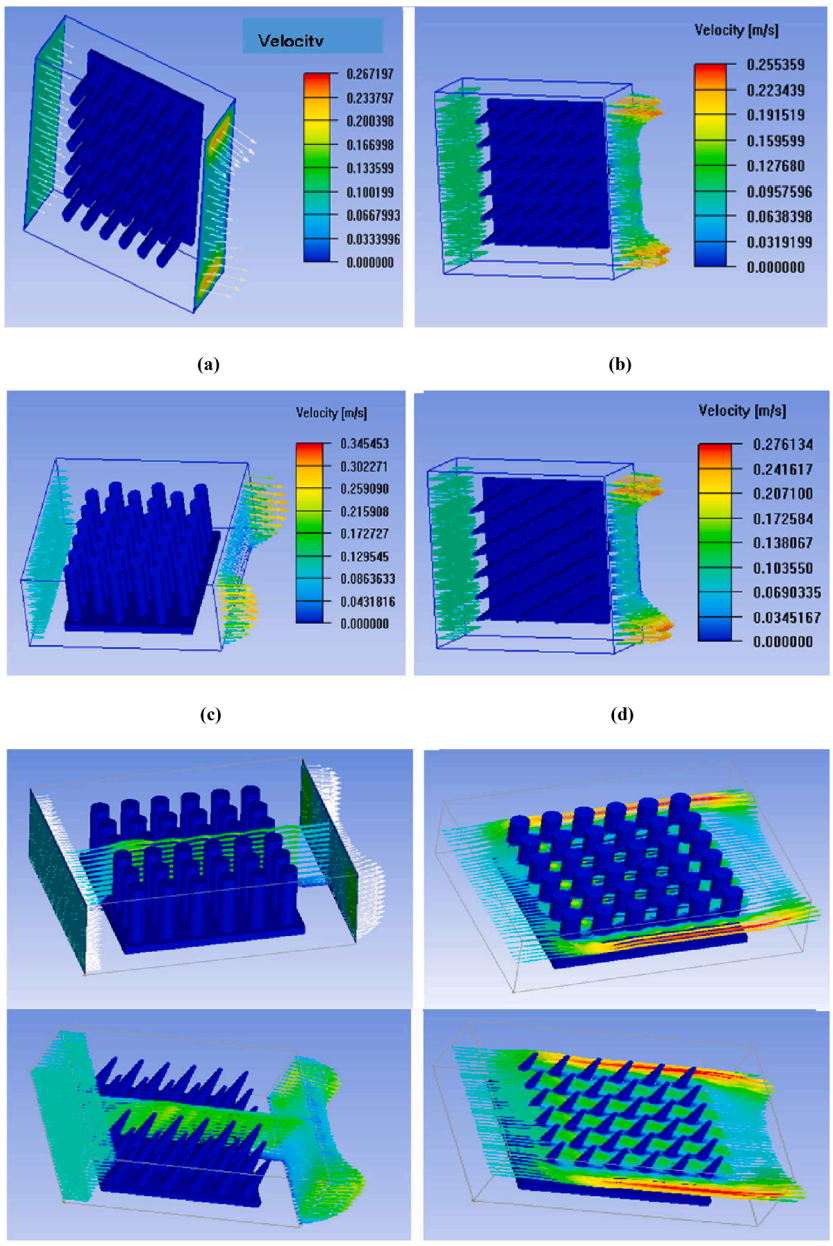

Fig. 11. Velocity contours of (a) circular IA fins (b) conical IA fins (c) circular SA fins (d) conical SA fins and (e) shows different views on streamlining the flow.

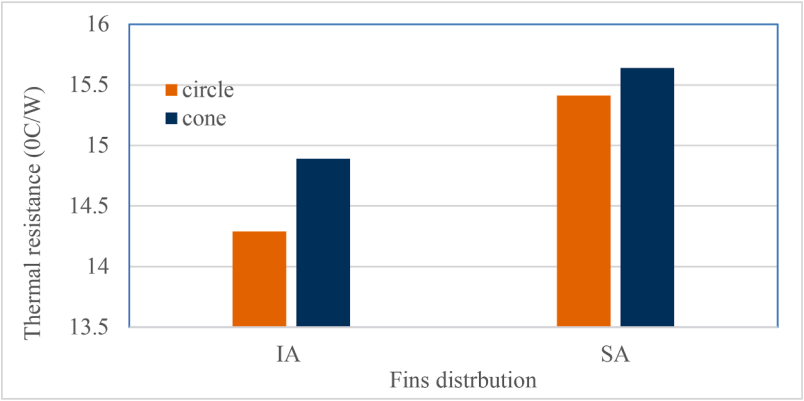

Fig. 12. The effect of fin cross-section and arrangement on the thermal resistance of a heat sink.

Table 6
The results for sources temperature for cone and circular in cases of IA and SA.

Arrangement	Source Temp (Circular)	Source Temp (Conical)
Inline (IA)	126.97 °C	128.65 °C
Staggered (SA)	125.50 °C	126.08 °C

Table 7
Summarises the pressure drop results for the cone and circular cases of IA and SA.

Arrangement	Pressure Drop (Circular)	Pressure Drop (Conical)
Inline (IA)	0.12	0.090
Staggered (SA)	0.16	0.10

surface area than conical fins for the same dimensions; the thermal resistance of a heat sink decreases with increasing area provided by finned metal devices, so the circular fins give low thermal resistance.

This study reveals a captivating relationship between the shape and layout of fins, which affects both heat transfer efficiency and pressure drop. The analysis is based on temperature and pressure data from Tables 4 and 6. When comparing cone fins to circular fins, it was consistently observed that circular fins had lower peak temperatures (up to 0.46% lower for staggered fins). This insight is directly relevant to the concept of surface area. The greater, uninterrupted surface area of round fins enables more efficient heat dispersion from the source to the surrounding fluid [23]. On the other hand, conical fins have a limited ability to transfer heat, resulting in elevated maximum temperatures due to their naturally smaller and more focused surface area.

Moreover, the staggered design is the most effective in reducing peak temperatures for both fins. Compared to the inline arrangement, the staggered configuration achieves reductions of up to 1.17% and 2.04% for circular and conical fins. This benefit stems from the disruptive impact of staggered fins on airflow. The fins, arranged in a staggered manner, function as barriers that compel the fluid to follow a longer and more convoluted route before reaching the outlet. This elongated flow channel substantially augments the overall surface area for heat transfer in contact with the fluid. By extending the duration of exposure, the heat dissipation from the fins becomes more effective, reducing the maximum temperature reached. This discovery emphasises the significance of including flow route optimisation into the heat exchanger design to enhance heat transfer efficiency.

Nevertheless, the advantages of the staggered layout are accompanied by the price. Table 7 demonstrates a persistent pattern of increased pressure drop for circular fins compared to conical fins, regardless of whether they are arranged inline or staggered. This difference arises from the underlying principles of fluid dynamics. The circular design creates a greater impediment to the flow, leading to increased resistance and a subsequent rise in pressure drop. In contrast, the sleek shape of the conical fins results in reduced flow resistance, which in turn leads to a decrease in pressure drop. The balance between heat transfer efficiency, which is improved by increasing the surface area, and the reduction of pressure drop, achieved by using streamlined designs, requires careful attention when designing fins. The selection of the most suitable fin geometry and arrangement is contingent upon the specific goals of the given application. In cases where it is crucial to maximise heat dissipation, circular fins or a staggered configuration may be favoured despite the resulting decrease in pressure. On the other hand, applications that are important in reducing flow resistance may prefer conical fins or a configuration where the fins are placed in a straight line.

4. Conclusion

This study investigates the effects of the shape of the fins and the way they are arranged on the performance of the microelectronic heat sink, as it used two types of arrangements: circular and conical fins arranged inline and staggered. ANSYS ICEPAK was used for numerical analysis, examining each case's temperature distribution and pressure drop. The study also seeks to offer a deeper understanding of the flow and heat transfer mechanisms within the fins. The most essential items extracted from this study are:

- The staggered arrangement significantly reduces peak temperatures (up to 2.04% for cone fins) compared to the inline arrangement, where the fluid travels a longer path and maximizes heat removal in a staggered arrangement.
- Circular fins outperform conical fins in heat dissipation due to their larger surface area, achieving up to 0.46% lower peak temperatures (especially in staggered arrangements).
- The type of application in which the fins are to be used may be the deciding factor in determining the type and shape of the arrangement. Although the staggered arrangement is preferred over the inline arrangement in a microelectronic heat sink, this may differ in other applications where it is superior in heat transfer; it comes at the cost of increased pressure drop. Circular fins, in particular, face a higher pressure drop penalty due to their shape, creating more flow resistance.
- The results of this study can give engineers light for designing fins that optimize performance based on specific application requirements.

CRediT authorship contribution statement

Sana J. Yaseen: Investigation, Data curation. **Zainab K. Radhi:** Validation, Software. **Rana L. Natoosh:** Methodology, Investigation. **Raheem Al-Sabur:** Resources, Project administration. **Raad Z. Homod:** Methodology, Conceptualization. **Hayder I. Mohammed:** Writing – original draft, Visualization.

Declaration of competing interest

The authors declare that they have no known competing financial interests or personal relationships that could have appeared to influence the work reported in this paper.

Data availability

No data was used for the research described in the article.

References

[1] A. Alkhazaleh, F. Alnaimat, M.Y. Selim, B. Mathew, Liquid cooling of microelectronic chips using MEMS heat sink: thermohydraulic characteristics of wavy microchannels with pin-fins, Int. J. Thermofluids 18 (2023) 100313, https://doi.org/10.1016/j.ijft.2023.100313.
[2] P.M. Cuce, E. Cuce, Optimisation of configurations to enhance heat transfer from a longitudinal fin exposed to natural convection and radiation, Int. J. Low-Carbon Technol. 9 (4) (2014), https://doi.org/10.1093/ijlct/ctt005.
[3] M. Ekpu, Finite element analysis of the effect of fin geometry on thermal performance of heat sinks in microelectronics, J. Appl. Sci. Environ. Manag. 23 (11) (2020), https://doi.org/10.4314/jasem.v23i11.24.
[4] A. Alkhazaleh, F. Alnaimat, B. Mathew, Fluid flow and heat transfer behavior of a liquid based MEMS heat sink having wavy microchannels integrating circular pin-fins, Int. J. Thermofluids 20 (2023) 100480, https://doi.org/10.1016/j.ijft.2023.100480.
[5] M.W. Uddin, N.S. Sifat, Comparative study on hydraulic and thermal characteristics of minichannel heat sink with different secondary channels in parallel and counter flow directions, Int. J. Thermofluids 17 (2023) 100296, https://doi.org/10.1016/j.ijft.2023.100296.
[6] A. Gaikwad, A. Sathe, S. Sanap, A design approach for thermal enhancement in heat sinks using different types of fins: a review, Front. Thermal Eng. 2 (2023), https://doi.org/10.3389/fther.2022.980985.
[7] L. Donetti, S. Mauro, G. Sequenzia, M. Calabretta, A. Sitta, Effects of the pin-fins cooler roughness on the thermo-fluid dynamics performance of a SiC power module, Int. J. Thermofluids 22 (2024) 100609, https://doi.org/10.1016/j.ijft.2024.100609.

[8] S.A.B. Al-Omari, F. Mahmoud, Z.A. Qureshi, E. Elnajjar, The impact of different fin configurations and design parameters on the performance of a finned PCM heat sink, Int. J. Thermofluids 20 (2023) 100476, https://doi.org/10.1016/j.ijft.2023.100476.
[9] A. Kumar, U. Dasari, Manoj, K. Mondal, Thermal performance of perforated pin finned heat sinks: a simulation-based study, in: COMSOL Conference, 2018, p. 2018.
[10] E.M. Sparrow, J.W. Ramsey, C.A.C. Altemani, Experiments on Inline Pin Fin Arrays and Performance Comparisons with Staggered Arrays, J. Heat. Transfer. 102 (1) (Feb. 1980) 44–50, https://doi.org/10.1115/1.3244247.
[11] S.C. Siw, A.D. Fradeneck, M.K. Chyu, M.A. Alvin, The effects of different pin-fin arrays on heat transfer and pressure loss in a narrow channel, in: Proceedings of the ASME Turbo Expo, 2015, https://doi.org/10.1115/GT2015-43855.
[12] J.M. Jalil, A.H. Reja, A.M. Hadi, Numerical Investigation of Thermal Performance of Micro-Pin Fin with Different Arrangements, in: IOP Conference Series: Materials Science and Engineering, 2020, https://doi.org/10.1088/1757-899X/765/1/012037.
[13] Y. Xu, L. Li, J. Wang, Experimental and numerical investigations of the thermal–hydraulic characteristics of novel micropin-fin heat sinks, Int. J. Heat. Mass Transf. 209 (2023) 124079, https://doi.org/10.1016/j.ijheatmasstransfer.2023.124079.
[14] M. Boujelbene, J.M. Mahdi, H.S. Sultan, R.Z. Homod, A. Yvaz, I.S. Chatroudi, P. Talebizadehsardari, The potential of arc-shaped fins for expedited solidification in triplex-tube latent heat storage: parametric investigation, J. Build. Eng. 82 (2024) 108176, https://doi.org/10.1016/j.jobe.2023.108176.
[15] N.A. Qasem, A. Abderrahmane, A. Belazreg, O. Younis, R.Z. Homod, M. Oreijah, K. Guedri, Influence of tree-shaped fins to enhance thermal storage units, Int. Commun. Heat Mass Transfer 151 (2024) 107220, https://doi.org/10.1016/j.icheatmasstransfer.2023.107220.
[16] Y. Xu, L. Li, Z. Yan, Experimental investigations of the flow boiling characteristics of green refrigerants in a novel petaloid micropin-fin heat sink, Int. J. Heat. Mass Transf. 212 (2023) 124243, https://doi.org/10.1016/j.ijheatmasstransfer.2023.124243.
[17] A. Hosseinpour, M. Pourfallah, M. Gholinia, Analysis of phase change material (PCM) melting utilising environmentally friendly nanofluids in a double tube with spiral fins: a numerical study, Int. J. Thermofluids 22 (2024) 100620, https://doi.org/10.1016/j.ijft.2024.100620.
[18] G. Tanda, Heat transfer and pressure drop in a rectangular channel with diamond-shaped elements, Int. J. Heat. Mass Transf. 44 (18) (2001), https://doi.org/10.1016/S0017-9310(01)00018-7.
[19] R.Z. Homod, F.A. Abood, S.M. Shrama, A.K. Alshara, Empirical correlations for mixed convection heat transfer through a fin array based on various orientations, Int. J. Thermal Sci. 137 (2019) 627–639, https://doi.org/10.1016/j.ijthermalsci.2018.12.012.
[20] O. Ozbalci, A. Dogan, M. Asilturk, Heat Transfer Performance of Plate Fin and Pin Fin Heat Sinks Using Al2O3/H2O Nanofluid in Electronic Cooling, Processes 10 (8) (2022), https://doi.org/10.3390/pr10081644.
[21] A. Dewan, P. Patro, I. Khan, P. Mahanta, The effect of fin spacing and material on the performance of a heat sink with circular pin fins, in: Proceedings of the Institution of Mechanical Engineers, Part A: Journal of Power and Energy 224, 2010, https://doi.org/10.1243/09576509JPE750.
[22] S.H. Hashemi Karouei, M. Bagheri Shani, M. Sekaloo, S.H. Hosseini Eimeni, P. Pasha, D. Domiri Ganji, Computational modeling of magnetised hybrid nanofluid flow and heat transfer between parallel surfaces with suction/injection, Int. J. Thermofluids 22 (2024) 100613, https://doi.org/10.1016/j.ijft.2024.100613.
[23] G. Anjaneya, et al., Numerical simulation of microchannel heat exchanger using CFD, International J. Interactive Design Manufacturing (IJIDeM) (Jun. 2023), https://doi.org/10.1007/s12008-023-01376-8.
[24] R. Rosli, K.A. Mohd Annuar, F.S. Ismail, Optimal Pin Fin Heat sink Arrangement for Solving Thermal Distribution Problem, J. Adv. Res. Fluid Mech. Thermal Sciences ISSN 11 (1) (2015).
[25] V. Saravanan, D. Hithaish, C.K. Umesh, K.N. Seetharamu, Numerical investigation of thermo-hydrodynamic performance of triangular pin fin heat sink using nanofluids, Thermal Sci. Engineering Progress 21 (2021), https://doi.org/10.1016/j.tsep.2020.100768.
[26] Y.T. Yang, H. Sen Peng, Numerical study of thermal and hydraulic performance of compound heat sink, Numeri. Heat. Transf. a Appl. 55 (5) (2009), https://doi.org/10.1080/10407780902776405.
[27] M.A.H. Abdelmohimen, K. Almutairi, M.A. Elkotb, H.E. Abdelrahman, S. Algarni, Numerical Investigation of Using Different Arrangement Of Fin Slides On The Plate-Fin Heat Sink Performance, Thermal Science 25 (6) (2021), https://doi.org/10.2298/TSCI201004065A.
[28] F. Zhou, I. Catton, Numerical evaluation of flow and heat transfer in plate-pin fin heat sinks with various pin cross-sections, Numeri. Heat. Transf. a Appl. 60 (2) (2011), https://doi.org/10.1080/10407782.2011.588574.
[29] K. Yakut, N. Alemdaroglu, I. Kotcioglu, C. Celik, Experimental investigation of thermal resistance of a heat sink with hexagonal fins, Appl. Therm. Eng. 26 (17–18) (2006), https://doi.org/10.1016/j.applthermaleng.2006.03.008.
[30] N.Y. Godi, Novel approach to cooling microelectronics with complex fins configuration, Int. J. Thermofluids 21 (2024) 100559, https://doi.org/10.1016/j.ijft.2024.100559.
[31] M. Daadoua, B. Mathew, F. Alnaimat, Experimental investigation of pressure drop and heat transfer in minichannel with smooth and pin fin surfaces, Int. J. Thermofluids 21 (2024) 100542, https://doi.org/10.1016/j.ijft.2023.100542.
[32] H.M. Maghrabie, A. Olabi, A.H. Alami, M.A. Radi, F. Zwayyed, T. Salamah, T. Wilberforce, M.A. Abdelkareem, Numerical simulation of heat pipes in different applications, Int. J. Thermofluids 16 (2022) 100199, https://doi.org/10.1016/j.ijft.2022.100199.
[33] Y.C. Hou, K.S. Mohamed Sahari, L.Y. Weng, et al., Development of collision avoidance system for multiple autonomous mobile robots, Int. J. Adv. Robot. Syst. 17 (4) (2020), https://doi.org/10.1177/1729881420923967.
[34] F.A. Abood, Z.K. Radhi, A.K. Hadi, R.Z. Homod, H.I. Mohammed, MHD mixed convection of nanofluid flow Ag- Mgo/water in a channel contain a rotational cylinder, Int. J. Thermofluids 22 (2024) 100713, https://doi.org/10.1016/j.ijft.2024.100713.
[35] S.J. Yaseen, Numerical study of the fluid flow and heat transfer in a finned heat sink using Ansys Icepak, Open Engineering 13 (1) (2023), https://doi.org/10.1515/eng-2022-0440.
[36] B.N. Alhasnawi, B.H. Jasim, Jasim, et al., A Multi-Objective Improved Cockroach Swarm Algorithm Approach for Apartment Energy Management Systems, Information 14 (2023) 521, https://doi.org/10.3390/info14100521.
[37] R. Adhikari, D. Wood, M. Pahlevani, An experimental and numerical study of forced convection heat transfer from rectangular fins at low Reynolds numbers, Int. J. Heat. Mass Transf. 163 (2020) 120418, https://doi.org/10.1016/j.ijheatmasstransfer.2020.120418.